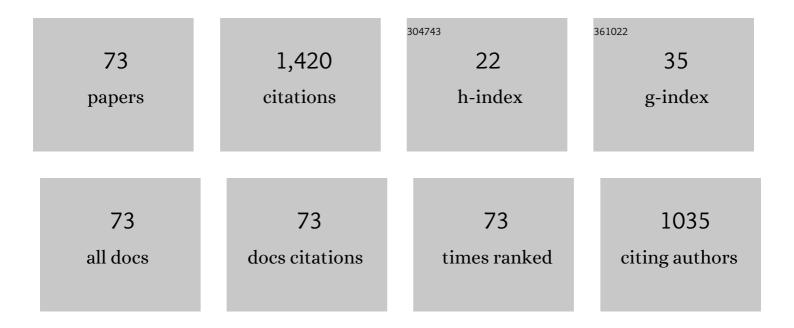
List of Publications by Year in descending order

Source: https://exaly.com/author-pdf/8738772/publications.pdf Version: 2024-02-01



IAN M HUIZENCA

#	Article	IF	CITATIONS
1	Quartz oxygen isotopes from Tick Hill area in Mount Isa Inlier: indication of a regional fluid overprint. Australian Journal of Earth Sciences, 2022, 69, 439-452.	1.0	1
2	Source and evolution of the ore-forming fluid of the Cuonadong Sn-W-Be polymetallic deposit (southern Tibet, China): Constraints from scheelite trace element and Sr isotope geochemistry. Ore Geology Reviews, 2022, 142, 104570.	2.7	11
3	Pre-Late Eocene position of the Lüchun-Jinping microblock in western Yangtze Craton: Constraints from Eocene-Oligocene lamprophyres in southeastern Tibet. Lithos, 2022, 414-415, 106622.	1.4	2
4	Petrogenesis of the quartz diorite from the Lietinggang-Leqingla Pb-Zn-Fe-Cu-(Mo) deposit in southern Tibet: Implications for the genesis of a skarn-type polymetallic deposit in the Tibetan-Himalayan collisional orogen. Ore Geology Reviews, 2022, 145, 104920.	2.7	0
5	Granitic magma evolution to magmatic-hydrothermal processes vital to the generation of HREEs ion-adsorption deposits: Constraints from zircon texture, U-Pb geochronology, and geochemistry. Ore Geology Reviews, 2022, 146, 104931.	2.7	6
6	Composition and evolution of the continental crust: Retrospect and prospect. Geoscience Frontiers, 2022, 13, 101428.	8.4	5
7	The Watershed Tungsten Deposit, Northeast Queensland, Australia: Permian Metamorphic Tungsten Mineralization Overprinting Carboniferous Magmatic Tungsten. Economic Geology, 2021, 116, 427-451.	3.8	6
8	Zircon <scp>U–Pb</scp> ages, geochemistry, and <scp>Sr–Nd–Pb–Hf</scp> isotopes of the Mugagangri monzogranite in the southern Qiangtang of Tibet, western China: Implications for the evolution of the Bangong <scp>Coâ€Nujiang Mesoâ€Tethyan</scp> Ocean. Geological Journal, 2021, 56, 3170-3186.	1.3	5
9	Generation and structural modification of the giant Kengdenongshe VMS-type Au-Ag-Pb-Zn polymetallic deposit in the East Kunlun Orogen, East Tethys: Constraints from geology, fluid inclusions, noble gas and stable isotopes. Ore Geology Reviews, 2021, 131, 104041.	2.7	7
10	Geological significance of Early Triassic porphyry Cu mineralization in the eastern Xar Moron–Changchun Metallogenic Belt, northeast China: A case study of the newly-discovered Guokuidingzi Cu deposit. Ore Geology Reviews, 2021, 133, 104092.	2.7	3
11	Petrology of the Machangqing Complex in Southeastern Tibet: Implications for the Genesis of Potassium-rich Adakite-like Intrusions in Collisional Zones. Journal of Petrology, 2021, 62, .	2.8	28
12	Rare earth element enrichment in the ion-adsorption deposits associated granites at Mesozoic extensional tectonic setting in South China. Ore Geology Reviews, 2021, 137, 104317.	2.7	13
13	Geological setting and mineralization characteristics of the Tick Hill Gold Deposit, Mount Isa Inlier, Queensland, Australia. Ore Geology Reviews, 2021, 137, 104288.	2.7	5
14	Constraining the genesis of tungsten mineralization in the Jiaoxi deposit, Tibet: A fluid inclusion and H, O, S and Pb isotope investigation. Ore Geology Reviews, 2021, 139, 104448.	2.7	7
15	Geochronological constraints on the geological history and gold mineralization in the Tick Hill region, Mt Isa Inlier. Precambrian Research, 2021, 366, 106422.	2.7	4
16	Mineralogical Characterization of Manganese Oxide Minerals of the Devonian Xialei Manganese Deposit. Minerals (Basel, Switzerland), 2021, 11, 1243.	2.0	0
17	40 Ar/ 39 Ar geochronology, fluid inclusions, and oreâ€grade distribution of the Jiawula Ag–Pb–Zn deposit, NE China : Implications for deposit genesis and exploration. Geological Journal, 2020, 55, 1115-1127.	1.3	7
18	Crustal thickening prior to 43 Ma in the Himalaya: Evidence from lower crustâ€derived adakitic magmatism in Dala, eastern Tethyan Himalaya, Tibet. Geological Journal, 2020, 55, 4021-4046.	1.3	14

#	Article	IF	CITATIONS
19	LA-ICP-MS trace element analysis of magnetite and pyrite from the Hetaoping Fe-Zn-Pb skarn deposit in Baoshan block, SW China: Implications for ore-forming processes. Ore Geology Reviews, 2020, 117, 103309.	2.7	32
20	Ore-fluid geochemistry of the Hehuashan Pb–Zn deposit in the Tongling ore district, Anhui province, China: Evidence from REE and C–H–O isotopes of calcite. Ore Geology Reviews, 2020, 117, 103279.	2.7	14
21	Trace element associations in magnetite and hydrothermal pyrite from the Geita Hill gold deposit, Tanzania. Journal of Geochemical Exploration, 2020, 209, 106418.	3.2	3
22	Reconstruction of an Early Permian, Sublacustrine Magmatic-Hydrothermal System: Mount Carlton Epithermal Au-Ag-Cu Deposit, Northeastern Australia. Economic Geology, 2020, 115, 129-152.	3.8	6
23	Mineralogical and isotopic characterization of graphite deposits in the western part of the North Qaidam Orogen and East Kunlun Orogen, northeast Tibetan Plateau, China. Ore Geology Reviews, 2020, 126, 103788.	2.7	5
24	Multi-stage crustal melting from Late Permian back-arc extension through Middle Triassic continental collision to Late Triassic post-collisional extension in the East Kunlun Orogen. Lithos, 2020, 360-361, 105446.	1.4	16
25	Geology, geochronology and geochemistry of the Miocene Jiaoxi quartz vein-type W deposit in the western part of the Lhasa Terrane, Tibet: Implications for ore genesis. Ore Geology Reviews, 2020, 120, 103433.	2.7	15
26	Formation of Late Cretaceous <scp>highâ€Mg</scp> granitoid porphyry in central Lhasa, Tibet: Implications for crustal thickening prior to India–Asia collision. Geological Journal, 2020, 55, 6696-6717.	1.3	9
27	Large-Scale Fluid Transfer between Mantle and Crust during Supercontinent Amalgamation and Disruption. Russian Geology and Geophysics, 2020, 61, 527-542.	0.7	4
28	TRACING CRUSTAL-SCALE FLUID PATHWAYS UNDER COVER WITH MAGNETOTELLURIC IMAGING. , 2020, , .		0
29	Chapter 8: The World-Class Gold Deposits in the Geita Greenstone Belt, Northwestern Tanzania. , 2020, , 163-183.		1
30	Fluid inclusion and stable isotope constraints on the heavy rare earth element mineralisation in the Browns Range Dome, Tanami Region, Western Australia. Ore Geology Reviews, 2019, 113, 103068.	2.7	4
31	Hypozonal orogenic gold mineralization in the Giyani Goldfield, Northern Kaapvaal Craton/Limpopo Complex. South African Journal of Geology, 2019, 122, 455-488.	1.2	4
32	Biotite chemistry and the role of halogens in Archaean greenstone hosted gold deposits: A case study from Geita Gold Mine, Tanzania. Ore Geology Reviews, 2019, 111, 102982.	2.7	6
33	The Neoarchaean Limpopo Orogeny: Exhumation and Regional-Scale Gravitational Crustal Overturn Driven by a Granulite Diapir. Regional Geology Reviews, 2019, , 185-224.	1.2	11
34	Vein-type graphite deposits in Sri Lanka: The ultimate fate of granulite fluids. Chemical Geology, 2019, 508, 167-181.	3.3	20
35	Delineating the structural controls on the genesis of iron oxide–Cu–Au deposits through implicit modelling: a case study from the E1 Group, Cloncurry District, Australia. Geological Society Special Publication, 2018, 453, 349-384.	1.3	9
36	The genesis of the Hehuashan Pb–Zn deposit and implications for the Pb–Zn prospectivity of the Tongling district, Middle–Lower Yangtze River Metallogenic Belt, Anhui Province, China. Ore Geology Reviews, 2018, 101, 105-121.	2.7	19

#	Article	IF	CITATIONS
37	Zircon U-Pb geochronology and geochemistry of the intrusions associated with the Jiawula Ag-Pb-Zn deposit in the Great Xing'an Range, NE China and their implications for mineralization. Ore Geology Reviews, 2017, 86, 35-54.	2.7	28
38	Alteration paragenesis and the timing of mineralised quartz veins at the world-class Geita Hill gold deposit, Geita Greenstone Belt, Tanzania. Ore Geology Reviews, 2017, 91, 765-779.	2.7	9
39	Composition and Evolution of Fluids Forming the Baiyinnuo'er Zn-Pb Skarn Deposit, Northeastern China: Insights from Laser Ablation ICP-MS Study of Fluid Inclusions*. Economic Geology, 2017, 112, 1441-1460.	3.8	93
40	The major and trace element chemistry of fish and lake water within major South African catchments. Water S A, 2016, 42, 112.	0.4	2
41	The strontium isotope distribution in water and sh within major South African catchments. Water S A, 2016, 42, 213.	0.4	3
42	High-temperature granulites and supercontinents. Geoscience Frontiers, 2016, 7, 101-113.	8.4	29
43	Vein graphite deposits: geological settings, origin, and economic significance. Mineralium Deposita, 2014, 49, 261-277.	4.1	72
44	Fluid-rock interaction during high-grade metamorphism: Instructive examples from the Southern Marginal Zone of the Limpopo Complex, South Africa. Precambrian Research, 2014, 253, 63-80.	2.7	24
45	Diamond formation by carbon saturation in C–O–H fluids during cold subduction of oceanic lithosphere. Geochimica Et Cosmochimica Acta, 2014, 143, 68-86.	3.9	52
46	Fluid-rock interaction in retrograde granulites of the Southern Marginal Zone, Limpopo high grade terrain, South Africa. Geoscience Frontiers, 2014, 5, 673-682.	8.4	25
47	Technical note: An inorganic water chemistry dataset (1972–2011) of rivers, dams and lakes in South Africa. Water S A, 2013, 39, .	0.4	4
48	Key factors controlling massive graphite deposition in volcanic settings: an example of a self-organized critical system. Journal of the Geological Society, 2012, 169, 269-277.	2.1	6
49	Diamond precipitation from ascending reduced fluids in the Kaapvaal lithosphere: Thermodynamic constraints. Comptes Rendus - Geoscience, 2012, 344, 67-76.	1.2	19
50	Granulites, CO2 and graphite. Gondwana Research, 2012, 22, 799-809.	6.0	50
51	Charnockite microstructures: From magmatic to metamorphic. Geoscience Frontiers, 2012, 3, 745-753.	8.4	47
52	Nature and origin of the protolith succession to the Paleoproterozoic Serra do Navio manganese deposit, Amapa Province, Brazil. Ore Geology Reviews, 2012, 47, 59-76.	2.7	22
53	Fluid-assisted granulite metamorphism: A continental journey. Gondwana Research, 2012, 21, 224-235.	6.0	79

#	Article	IF	CITATIONS
55	Granite emplacement and the retrograde P-T-fluid evolution of Neoarchean granulites from the Central Zone of the Limpopo Complex. , 2011, , .		5
56	Characterisation of the inorganic chemistry of surface waters in South Africa. Water S A, 2011, 37, .	0.4	10
57	Thermodynamic modelling of a cooling C–O–H fluid–graphite system: implications for hydrothermal graphite precipitation. Mineralium Deposita, 2011, 46, 23-33.	4.1	54
58	The graphite deposit at Borrowdale (UK): A catastrophic mineralizing event associated with Ordovician magmatism. Geochimica Et Cosmochimica Acta, 2010, 74, 2429-2449.	3.9	43
59	Deposition of highly crystalline graphite from moderate-temperature fluids. Geology, 2009, 37, 275-278.	4.4	75
60	The Paleoproterozoic carbonate-hosted Pering Zn–Pb deposit, South Africa. II: fluid inclusion, fluid chemistry and stable isotope constraints. Mineralium Deposita, 2006, 40, 686-706.	4.1	33
61	Carbonic fluid inclusions in Paleoproterozoic carbonate-hosted Zn-Pb deposits in Griqualand West, South Africa. South African Journal of Geology, 2006, 109, 55-62.	1.2	7
62	COH, an Excel spreadsheet for composition calculations in the C–O–H fluid system. Computers and Geosciences, 2005, 31, 797-800.	4.2	40
63	Geological and anthropogenic influences on the inorganic water chemistry of the Jukskei River, Gauteng, South Africa. South African Journal of Geology, 2005, 108, 439-447.	1.2	3
64	Structural and P-T Evolution of a Major Cross Fold in the Central Zone of the Limpopo High-Grade Terrain, South Africa. Journal of Petrology, 2004, 45, 1413-1439.	2.8	49
65	Fluids in granulites of the Southern Marginal Zone of the Limpopo Belt, South Africa. Contributions To Mineralogy and Petrology, 2001, 141, 529-545.	3.1	34
66	Thermodynamic modelling of C–O–H fluids. Lithos, 2001, 55, 101-114.	1.4	84
67	A Ni- and PCE-enriched quartz norite impact melt complex in the Late Jurassic Morokweng impact structure, South Africa. , 1999, , .		13
68	Fluid evolution in the Pote Shear Zone Harare-Shamva-Bindura greenstone belt (northeast Zimbabwe). Journal of African Earth Sciences, 1999, 28, 311-324.	2.0	0
69	Precambrian intraplate magmatism: high temperature, low pressure crustal granulites. Journal of African Earth Sciences, 1999, 28, 367-382.	2.0	30
70	Fluid inclusions in shear zones: The case of the Umwindsi shear zone in the Harare-Shamva-Bindura greenstone belt, NE Zimbabwe. European Journal of Mineralogy, 1999, 11, 1079-1090.	1.3	28
71	Fluids and eoigenetic gold mineralisation at Shamva Mine, Zimbabwe: a combined structural and fluid inclusion study. Journal of African Earth Sciences, 1998, 27, 55-70.	2.0	10
72	Topaz, Aquamarine, and Other Beryls from Klein Spitzkoppe, Namibia. Gems & Gemology, 1998, 34, 114-125.	0.6	6

#	Article	IF	CITATIONS
73	Infra-supra structure relations of a microcline-granite dome in the Somero area, Svecofennides, SW Finland. Bulletin of the Geological Society of Finland, 1989, 61, 131-141.	0.8	5